NORMAL MODES IN A CRYOGENIC PURE ION PLASMA

DANIEL H.E. DUBIN

Department of Physics, University of California at San Diego, La Jolla CA 92093-0319, USA

When a single species plasma is confined in a harmonic Penning trap at cryogenic temperature and high density a confined thermal equilibrium exists in which the plasma is roughly a uniform density spheroid (ellipsoid of revolution). Some of the normal modes of this magnetized plasma spheroid have recently been measured. Here, a simple electrostatic cold fluid theory of the modes is presented. Although the magnetized plasma dielectric is anisotropic (with cylindrical symmetry) and the plasma boundary has a different—spheroidal—symmetry, a separable analytic solution nevertheless exists in an unusual frequency-dependent coordinate system. Furthermore, those modes which correspond to quadrupole deformations of the spheroid have a simple finite amplitude description (and it is these modes which were measured in the experiments). Preliminary molecular dynamics simulation results exploring the effects of strong correlation on the normal mode frequencies will also be presented.

1. INTRODUCTION

In recent experiments[1] a nonneutral plasma is confined for long periods of time in a Penning trap. The plasma is at sufficiently low temperature T and sufficiently high density n_0 so that both the Debye length $\lambda_D=(kT/4\pi q^2 n_0)^{1/2}$ and the interparticle spacing $n_0^{-1/3}$ are much smaller than the size of the plasma (here q is the ion charge). However, the plasma is itself much smaller than the distance to the trap electrodes, so that induced image charges in the electrodes have a negligible effect on the plasma dynamics.

Normal modes have recently been excited and measured in such a plasma cloud.[2] This paper describes a simple analytic theory for these modes. Although the magnetized plasma dielectric is anisotropic (with cylindrical symmetry) and the plasma is also bounded (with a different—spheroidal—symmetry), we show that a separable solution for the partial differential equation governing the mode potential exists, and we obtain an analytic solution for electrostatic fluid modes in a realistic confined nonneutral plasma of finite size. We also report on the preliminary results of some computer simulations which have been performed in order to test the theory and which also may be able to provide information on the viscosity of the strongly correlated plasma.

The confinement properties of nonneutral plasmas in Penning traps have been studied extensively. Radial confinement is maintained by a strong uniform magnetic field B oriented along the trap axis (taken here to be the z direction). The plasma rotates through this magnetic field, providing a confining $\mathbf{v}\times\mathbf{B}$ force which balances the repulsive radial electric force of the unneutralized plasma. Confinement in the z direction is provided by DC voltages applied to end electrodes. The assumption that the plasma is small implies that image charges in the electrodes can be neglected and the trap potential is approximately quadratic, of the form $z^2-(x^2+y^2)/2$. A single particle trapped in this potential oscillates in the z direction at frequency ω_z, the single particle axial bounce frequency.

Furthermore, the existence of a confined thermal equilibrium state for plasmas confined in such a trap has been demonstrated both theoretically[3] and experimentally.[4,5] In thermal equilibrium, the plasma rotates with a uniform "rigid" rotation frequency ω_r, and is at constant temperature T. If both λ_D and $n_0^{-1/3}$ are much less than the size of the plasma, one may neglect the effects of finite temperature and correlations and the resulting cold fluid thermal equilibrium is a uniform density spheroid (ellipsoid of revolution) whose aspect ratio α determines the cloud's rotation frequency ω_r for given trap fields (see Eq. (15) of Ref. 5). (The aspect ratio α is defined in terms of the cloud's axial length, $2z_0$, and its diameter, $2r_0$, as $\alpha=z_0/r_0$.) The rotation frequency in turn is related to the density[3] by $\omega_p^2=2\omega_r(\Omega-\omega_r)$, where $\Omega=qB/Mc$ is the cyclotron frequency, $\omega_p=\sqrt{4\pi q^2 n_0/M}$ is the plasma frequency, and M is the mass of the charges in the plasma.

2. FLUID DESCRIPTION OF THE NORMAL MODES

In order to obtain a general solution for the normal modes several assumptions must be made. We assume the cloud is near thermal equilibrium, and we assume the oscillations around this equilibrium are small so that we can linearize the equations of motion. The temperature is assumed to be sufficiently small so that pressure effects

on the fluid dynamics are negligible, and correlation effects are also neglected; these are good approximations provided that both the Debye length and interparticle spacing are small compared to both the size of the cloud and the wavelength of the mode. Electromagnetic effects are neglected since the cloud is small and the mode frequency is relatively low, and the effect on the dynamics of image charges in the electrodes is neglected.

These approximations apply well to present experiments on small cold ion clouds. The equations of motion consistent with these approximations are the cold fluid equations linearized around the $T=0$ spheroidal fluid thermal equilibrium. The dynamics is described in a frame rotating with the plasma. In this frame the equilibrium is stationary and the perturbed density δn, velocity $\delta \mathbf{v}$ and electrostatic potential ψ satisfy the linearized continuity, momentum and Poisson equations:

$$\frac{\partial \delta n}{\partial t} + \nabla \cdot (n_0 \delta \mathbf{v}) = 0 \tag{1a}$$

$$\frac{\partial \delta \mathbf{v}}{\partial t} + \frac{q}{M} \nabla \psi - \delta \mathbf{v} \times \Omega_v \hat{\mathbf{z}} = 0 \tag{1b}$$

$$\nabla^2 \psi = -4\pi q \, \delta n \tag{1c}$$

where $\Omega_v = \Omega - 2\omega_r$ is the vortex frequency (the cyclotron frequency as seen in the rotating frame), and $\hat{\mathbf{z}}$ is a unit vector in the z-direction. Using the ansatz that the perturbed quantities have a time dependence of the form $e^{-i\omega t}$ in the rotating frame (so that ω is the mode frequency as seen in this frame), a differential equation for ψ follows from standard algebraic manipulations of Eqs. (1):

$$\nabla \cdot \boldsymbol{\varepsilon} \cdot \nabla \psi = 0 \tag{2a}$$

where $\boldsymbol{\varepsilon}$ is the cold plasma dielectric tensor. In Cartesian coordinates

$$\boldsymbol{\varepsilon} = \begin{bmatrix} \varepsilon_1 & -i\varepsilon_2 & 0 \\ i\varepsilon_2 & \varepsilon_1 & 0 \\ 0 & 0 & \varepsilon_3 \end{bmatrix} \tag{2b}$$

where $\varepsilon_1 = 1 - \omega_p^2/(\omega^2 - \Omega_v^2)$, $\varepsilon_2 = \Omega_v \omega_p^2/\omega(\omega^2 - \Omega_v^2)$ and $\varepsilon_3 = 1 - \omega_p^2/\omega^2$. Equation (2a) is just Maxwell's equation $\nabla \cdot \mathbf{D} = 0$ for a medium with a linear frequency-dependent anisotropic dielectric tensor $\boldsymbol{\varepsilon}$.

The normal mode problem requires a solution to this equation subject to the boundary condition that $\psi \to 0$ at infinity, which is a problem in the theory of electrostatics. Outside the plasma $\varepsilon = 1$ and ψ satisfies Laplace's equation, $\nabla^2 \psi^{out} = 0$. Inside the plasma the dielectric tensor is anisotropic and the solution of Eq. (2a) is more complicated. The inner and outer solutions must be matched across the plasma-vacuum boundary according to

$$\psi^{in} = \psi^{out} \Big|_{boundary} , \tag{3a}$$

$$\hat{\mathbf{n}} \cdot \boldsymbol{\varepsilon} \cdot \nabla \psi^{in} = \hat{\mathbf{n}} \cdot \nabla \psi^{out} \Big|_{boundary} , \tag{3b}$$

where $\hat{\mathbf{n}}$ is a unit vector normal to the plasma vacuum boundary.

The formulation of the problem as one in the theory of electrostatics is a step forward, but is hardly the end of the story. Although the problem is well-posed, simple solutions are generally available only in one of the standard geometries for which a separable solution exists, and this is not such a case. The surface of the plasma is spheroidal, while the dielectric tensor is anisotropic with a different, cylindrical, symmetry. However, in Ref. 6 it was shown that Eq. (2) does in fact have a separable solution in an unusual frequency dependent coordinate system. This is the only known exact analytic solution for normal modes in a magnetized plasma of finite size. The solution for the mode potential is

$$\psi = \begin{cases} A \, Q_l^m(\xi_1/d) \, P_l^m(\xi_2) \, e^{i(m\phi - \omega t)} & \text{(outside cloud)} \\ B \, P_l^m(\bar{\xi}_1/\bar{d}) \, P_l^m(\bar{\xi}_2) \, e^{i(m\phi - \omega t)} & \text{(inside cloud)} \end{cases} \tag{4}$$

where A and B are constants and Q_l^m and P_l^m are associated Legendre functions. Outside the cloud the solution is expressed in terms of spheroidal coordinates (ξ_1, ξ_2, ϕ) defined by the relations

$$x = [(\xi_1^2 - d^2)(1 - \xi_2^2)]^{1/2} \cos\phi \ ,$$

$$y = [(\xi_1^2 - d^2)(1-\xi_2^2)]^{1/2}\sin\phi \ ,$$

$$z = \xi_1\xi_2 \ .$$

The coordinate ξ_1 is a generalized distance coordinate taking the values $\xi_1 \varepsilon [z_0,\infty)$ outside the cloud, ξ_2 is a generalized latitude in the range [-1,1] and ϕ is the usual azimuthal angle. Surfaces of constant ξ_1 are confocal spheroids with the surface of the cloud defined by $\xi_1 = z_0$, and surfaces of constant ξ_2 are confocal hyperboloids. The focii are a distance $2|d|$ apart, and $d^2 \equiv z_0^2 - r_0^2$. The coordinates (ξ_1,ξ_2,ϕ) become the usual spherical coordinates $(r,\cos\theta,\phi)$ when $z_0 = r_0$.

Inside the cloud the coordinates $(\bar{\xi}_1, \bar{\xi}_2, \phi)$ are employed in order to obtain a separable solution. These coordinates are transformed spheroidal coordinates defined by the equations

$$\begin{aligned} x &= [(\bar{\xi}_1^2 - \bar{d}^2)(1-\bar{\xi}_2^2]^{1/2}\cos\phi \ , \\ y &= [(\bar{\xi}_1^2 - \bar{d}^2)(1-\bar{\xi}_2^2]^{1/2}\sin\phi \ , \\ z(\varepsilon_1/\varepsilon_3)^{1/2} &= \bar{\xi}_1\bar{\xi}_2 \end{aligned} \tag{5}$$

where $\bar{d}^2 = \bar{z}_0^2 - r_0^2$ and $\bar{z}_0 = z_0(\varepsilon_1/\varepsilon_3)^{1/2}$. These coordinates are frequency-dependent; the different possible topologies of the coordinate surfaces are discussed in Ref. 6.

Returning to Eq. (4), we note that different normal modes are enumerated by the integers l and m, where $l \geq 0$ and $|m| \leq l$. In fact, values of m less than zero do not give rise to new modes so $m \geq 0$ is assumed throughout, and negative frequencies are allowed. Negative frequencies have the following interpretation. For $m \neq 0$, positive and negative frequency modes rotate about the z axis in opposite directions. We choose the convention that modes with positive frequency rotate in the counter-clockwise sense when viewed from above the x-y plane (so that $d\theta/dt > 0$ for $\omega > 0$). These two directions of rotation are not equivalent due to the applied magnetic field.

For a given pair (l,m) the mode potential outside the cloud decays away like $s^{-(l+1)}$ at large distances s from the cloud center (because $Q_l^m(x) \to x^{-(l+1)}$ for large x and $\xi_1 \to s$ for large s). The modes can also be differentiated by the number of oscillations in ψ. For example, there are $l-m$ zeroes in the potential as one moves in ξ_2 along a given spheroid from one pole to the other (i.e., from $\xi_2 = 1$ to -1 on a constant (ξ_1,ϕ) curve). This is because $P_l^m(x)$ has $l-m$ zeroes in the range [-1,1].

For a given pair (l,m) there are several possible frequencies of oscillation which we will enumerate presently. The variation of the potential outside the cloud is independent of the mode frequency, up to the overall constant A. However, inside the cloud, the frequency dependence of the coordinates (through their dependence on ε_1 and ε_3) implies that the behavior of the mode potential varies depending on the mode frequency, the plasma frequency and vortex frequency (except for two exceptional cases described by Eqs. (8) and (9) below). This behavior can be understood qualitatively from the spatial Fourier transform of Eq. (2a),

$$\varepsilon_1 k_\perp^2 + \varepsilon_3 k_z^2 = 0 \ , \tag{6}$$

where $\mathbf{k}_\perp$ and k_z are the components of wave vector perpendicular and parallel to the magnetic field respectively. When ω/ω_p and Ω_v/ω_p are such that $\varepsilon_1/\varepsilon_3 < 0$, a solution of this equation exists with both $\mathbf{k}_\perp$ and k_z real, which is a propagating mode. As the mode reflects off the cloud's surface it sets up a standing wave pattern of nodes and antinodes within the plasma. As an example, the zeroes of the potential for the four possible $l=4$ $m=0$ potentials are shown in Fig. 1 for the case of a spherical plasma with $\Omega_v/\omega_p = 0.5$. Note that the zeroes of the mode intersect the surface of the cloud at the same points for all four frequencies since in all cases the potential outside the cloud varies like $P_4^0(\cos\theta)$, and is continuous across the plasma vacuum boundary.

The relation $\varepsilon_1/\varepsilon_3 < 0$ is satisfied by frequencies in the ranges $0 < |\omega| < \min[\omega_p, |\Omega_v|]$ and $\max[\omega_p, |\Omega_v|] < |\omega| < \Omega_u$ where $\Omega_u = \sqrt{\omega_p^2 + \Omega_v^2}$ is the upper hybrid frequency. Propagating modes in the former range are called magnetized plasma oscillations, whereas modes in the latter range are referred to as upper hybrid modes. Figures 1a and 1b are upper hybrid modes and 1d is a magnetized plasma mode. Figure 1c corresponds to the case of a mode with $\varepsilon_1/\varepsilon_3 > 0$, which we discuss below. The two (4,0) upper hybrid modes induce little potential variation outside the cloud when $|\Omega_v| < \omega_p$, and so may be difficult to observe in this regime if only electrostatic probes are employed. This is because at the "Brillouin limit" defined by $\Omega_v = 0$, these modes become bulk plasma oscillations with $\varepsilon_3 = 0$, and so Eq. (3) implies that $\psi^{out} = 0$. Furthermore, at the Brillouin limit the magnetized plasma modes disappear into the $\omega = 0$ resonance. Thus, only modes with $\varepsilon_1/\varepsilon_3 > 0$ may be observable near this limit (under electrostatic detection).

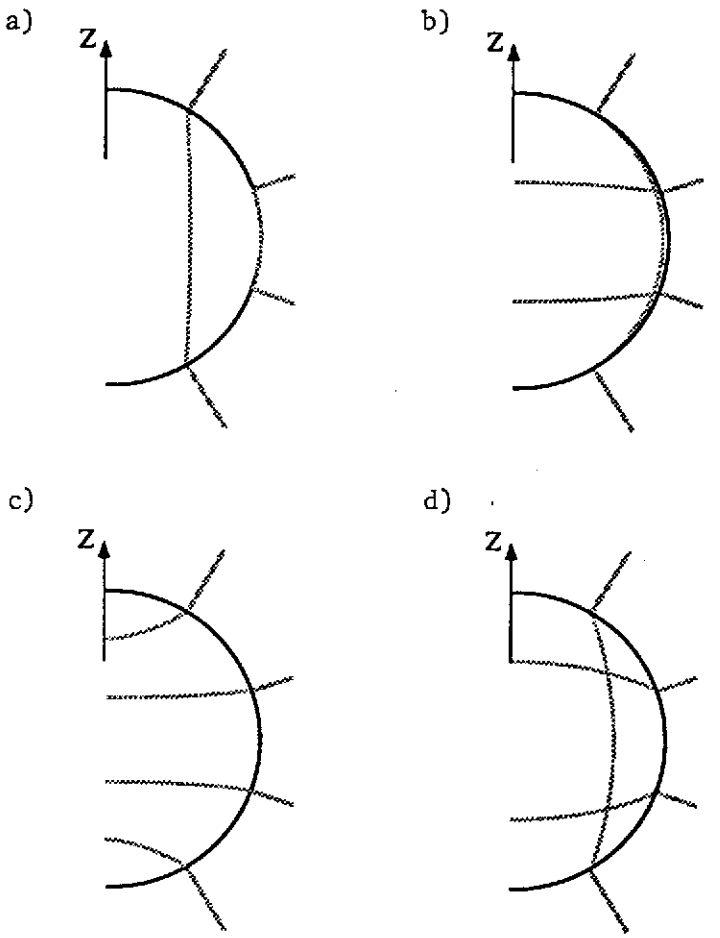

FIGURE 1

Figures a — d show the zeroes of the potential for the four $l=4$, $m=0$ modes in a spherical plasma cloud with $\Omega_v/\omega_p = 1/2$, in order of highest frequency to lowest frequency. Grey lines are the zeroes, and the black line is the surface of the cloud.

When $\varepsilon_1/\varepsilon_3 > 0$, Eq. (6) implies that both k_1 and k_z can no longer be real and the mode is evanescent, decaying with distance into the plasma. There are in general two such modes when $|\Omega_v| < \omega_p$, with frequencies in the range $|\Omega_v| < |\omega| < \omega_p$ (when $m=0$ the two modes are degenerate, so only one, labelled c, is shown in Fig. 1). Furthermore, if $\varepsilon_1 = \varepsilon_3$ (which can occur only at the Brillouin limit $\Omega_v = 0$) these evanescent modes satisfy $\nabla^2\psi^{in} = 0$, which from Eq. (1c) implies that there is no density perturbation except at the surface of the cloud. In this case the evanescent modes induce incompressible deformations of the cloud's shape, and for this reason such modes are often referred to as surface modes.

Finally, there are two exceptional cases for which the form of the interior mode potential is independent of ω, ω_p and Ω_v. When $l=m$ or $l=m+1$ one can substitute into Eq. (4) the general form of the Legendre function P_l^m,

$$P_l^m(x) = \sum_{j=0}^{(l-m)/2} (1-x^2)^{\frac{m}{2}} p_{lmj} x^{l-m-2j} \ , \tag{7}$$

(where the p_{lmj}'s are given numbers), and use Eq. (5) to show that

$$\psi^{in}_{(m,m)} = \bar{A} r^m e^{i(m\phi - \omega t)} \tag{8}$$

and

$$\psi^{in}_{(m+1,m)} = \bar{B} r^m z\, e^{i(m\phi-\omega t)} \quad , \tag{9}$$

where $\bar{A}$ and $\bar{B}$ are constants. In these cases the form of the mode potential is independent of ω, ω_p and Ω_v because the mode satisfies $\partial^2\psi^{in}/\partial z^2 = 0$ and $\nabla_\perp^2\psi^{in} = 0$ separately, and so Eq. (2a) is satisfied for any ε_1 and ε_3. (In fact, for all l and m ψ^{in} can be expressed as a finite-order multinomial in x, y and z.) Furthermore, these particular modes satisfy $\nabla^2\psi^{in} = 0$, so they cause incompressible deformations of the cloud for all ω_p and Ω_v, i.e., they are always surface modes. For example, for the case of the (2,1) mode $\psi^{in}_{(2,1)} = \bar{B}\, e^{i(\phi-\omega t)} r\, z$, which is the potential inside a tilted cloud precessing at frequency ω around the z axis. The (1,0) and (1,1) modes are also examples of incompressible cloud deformations, which correspond to the well-known axial center of mass and magnetron modes.

The (2,2) mode is also an incompressible distortion of the cloud, in this case into a triaxial ellipsoid. The ellipsoid then rotates about the z axis at one of two possible frequencies. In fact, all the $l = 2$ modes correspond to distortions of the plasma into a time varying ellipsoidal figure. A simple finite amplitude theory of these particular modes has recently been developed.[7] Furthermore, the (l,l) modes are finite length extensions of the z-independent diocotron and upper hybrid surface modes of cylindrical nonneutral plasmas.[8]

Although the $l = m$ and $l = m+1$ surface modes appear to be fundamentally different from other magnetized plasma, upper hybrid, and evanescent modes, in fact they display many characteristics which are similar to these modes. For example, one of the three (2,1) oscillations can be thought of as the finite length version of a magnetized plasma mode in a cylindrical column. The mode has $m = 1$ and has half a wavelength potential variation over the length of the column. Similarly, the other two (2,1) modes are finite length versions of diocotron and upper hybrid oscillations which also have a half-wavelength variation over the column length. Modes with larger values of l simply have more wavelengths fitted into the column length, and so are not fundamentally different. Indeed, we will soon see that the frequencies of these $l = m$ and $l = m+1$ modes behave in a qualitatively similar fashion as those of the other propagating and evanescent modes. When discussing the general frequency dependence of the modes, we therefore need make no distinction between these modes and modes with other values of l and m.

Turning now to the normal mode frequencies, in Ref. 6 it was shown that substitution of Eq. (4) into Eq. (5) leads to two homogeneous linear equations for A and B which have a nontrivial solution only if

$$\varepsilon_3 P_l^{m\prime} + m\alpha\left[\alpha^2 - \frac{\varepsilon_3}{\varepsilon_1}\right]^{1/2} P_l^m \varepsilon_2 - \left[\frac{\alpha^2 - \varepsilon_3/\varepsilon_1}{\alpha^2 - 1}\right]^{1/2} P_l^m \frac{Q_l^{m\prime}}{Q_l^m} = 0 \, , \tag{10}$$

where $P_l^m = P_l^m(\alpha/(\alpha^2 - \varepsilon_3/\varepsilon_1)^{1/2})$, $Q_l^m = Q_l^m(\alpha/(\alpha^2-1)^{1/2})$, $\alpha = z_0/r_0$, and the primes denote differentiation with respect to the entire argument.

The general behavior of the solutions to this equation was considered in Ref. 6. Here, we discuss a simplification of Eq. (10) which aids in the determination of the solutions. Analysis of the roots of this nonlinear equation is aided by the fact that it can be expressed as a polynomial in the frequency ω. This polynomial can be derived by substitution of Eq. (7) into Eq. (10), which leads, after some algebra, to the expression

$$x^{l-m-1}(1-x^2)^{\frac{m}{2}} \sum_{j=0}^{\frac{l-m}{2}} p_{lmj} x^{-2j} \left[m\alpha^2(\varepsilon_1+\varepsilon_2) + (l-m-2j)\varepsilon_3 - \frac{\alpha}{(\alpha^2-1)^{1/2}} \frac{Q_l^{m\prime}}{Q_l^m} \right] = 0 \, , \tag{11}$$

where $x = \alpha/(\alpha^2 - \varepsilon_3/\varepsilon_1)^{1/2}$. The prefactor of the sum is nonzero and so can be discarded. Furthermore, since $x^{-2j} = (1 - \varepsilon_3/\alpha^2\varepsilon_1)^j$, and ε_1, ε_2 and ε_3 are rational functions of ω, the sum itself may be expressed as a polynomial in ω. For example, $\varepsilon_3/\varepsilon_1 = (\omega^2 - \Omega_v^2)(\omega^2 - \omega_p^2)/\omega^2(\omega^2 - \Omega_u^2)$, and $\varepsilon_1 + \varepsilon_2 = (\omega^2 + \omega\Omega_v - \omega_p^2)/\omega(\omega + \Omega_v)$. Substitution of these results into Eq. (11) leads, after some further reduction, to the following polynomial equation:

$$\sum_{j=0}^{(l-m)/2} a_j\, b^j\, c^{Int[(l-m)/2]-j} = 0 \, , \tag{12}$$

where

$$a_j = p_{lmj} \left\{ (\omega+\Omega_v)\left[(l-m-2j)(\omega^2-\omega_p^2) - \frac{\alpha}{(\alpha^2-1)^{1/2}} \frac{Q_l^{m\prime}}{Q_l^m} \omega^2 \right] \right.$$

$$\left. + m\alpha^2\omega(\omega^2 - \omega_p^2 + \omega\Omega_v) \right\} \, ,$$

$$b = \alpha^2\omega^2(\omega^2-\Omega_u^2)-(\omega^2-\omega_p^2)(\omega^2-\Omega_v^2)\ ,$$

and

$$c = \alpha^2\omega^2(\omega^2-\Omega_u^2)\ .$$

This form of the dispersion relation is considerably simpler to solve numerically than Eq. (10) using any polynomial root finding algorithm. Furthermore, the equation leads to some simple analytic results. For example, one can count the number of normal modes by determining the order of the polynomial. One can see that the order is $3+4\,Int[(l-m)/2]$; however, one must be careful to exclude any spurious roots generated in the derivation of Eq. (12) through multiplication by resonant denominators of ε_1, ε_2 or ε_3. When $m=0$ and l is odd there is a single spurious root at $\omega=-\Omega_v$ (due to the $(\omega+\Omega_v)$ term in a_j). If $m=0$ and l is even there are three spurious roots at $\omega^2=0$ and $\omega=-\Omega_v$. Subtracting out these roots from the total, one finds for $m=0$ there are $2l$ normal modes. However, when $m=0$ Eq. (12) is a polynomial of order l in ω^2. The roots then come in l pairs at $\pm\omega$, and the pairs do not really correspond to two separate modes; indeed, Eq. (4) shows that the mode potential is identical for both $\pm\omega$ when $m=0$.

When $m\neq 0$ and when $l=m$ is even, there is a single spurious root at $\omega=0$, while when $l-m$ is odd there are no spurious roots. Thus, when $l-m$ is even there are $2(l-m)+2$ modes, and when $l-m$ is odd there are $2(l-m)+1$ modes. The roots no longer come in $\pm\omega$ pairs because, for $m\neq 0$, modes with positive and negative frequencies rotate in opposite directions around the z-axis, and these directions are not equivalent because of the magnetic field.

3. THE EFFECT OF STRONG CORRELATION: PRELIMINARY RESULTS

In order to determine the effect of interparticle correlations on the normal modes we have performed molecular dynamics computer simulations of ion clouds in which an oscillation has been induced.[9] The molecular dynamics code follows the orbits of N charges under the influence of the external electric and magnetic fields as well as the Coulomb interactions with the other charges. In order to remove the fast cyclotron timescale from the dynamics we analytically average over the cyclotron motion, replacing the exact equations of motion by guiding center equations of motion. The idea here is that for a sufficiently strong magnetic field the cyclotron motion decouples from the motions associated with normal modes at or below the plasma frequency. Details of the molecular dynamics method can be found in Ref. 10. Each particle is described by a position $\mathbf{x}_i$ and velocity along the magnetic field, v_{zi} (the other two components of velocity are determined by the $\mathbf{E}\times\mathbf{B}$ drift).

We begin the simulation by using for an initial condition the positions $\mathbf{x}_i^{(0)}$ and velocities $v_{zi}^{(0)}$ of charges which have previously been allowed to equilibrate to some value of the correlation parameter $\Gamma\equiv e^2/akT$. We determine the temperature as a long-time average of the mean kinetic energy [i.e., $T=\langle(1/N)\sum_i M v_{zi}^2\rangle$]. As is the practice in OCP studies, we calculate the Wigner-Seitz radius a in terms of the background density (that is, $\frac{4}{3}\pi a^3 n_0=1$, where n_0 is determined in the simulations from the time average of the rotation frequency [i.e., $n_0=(B/2\pi ec)\langle\omega_r\rangle$]).

To these positions and velocities we add a perturbation associated with a given normal mode. The mode fluid velocities and displacements can be obtained from Eq. (4). We then follow the evolution of the plasma through several oscillations in order to determine the mode frequency and to observe collisional damping of the mode. Some results are shown in Fig. 2 for a cloud of $N=768$ particles which is initially spherical ($\alpha=1$). In order to simulate a (2,0) mode we add to each particle's velocity a small component proportional to z:

$$\mathbf{x}_i(t=0)=\mathbf{x}_i^{(0)}\ ,$$

$$v_{zi}(t=0)=v_{zi}^{(0)}+0.05z_i^{(0)}\ ,\ i=1-N\ .$$

This mode corresponds to a sinusoidal oscillation in the length of the spheroid. The radius of the plasma is constant because we use guiding center dynamics for which the mean square radius, $\sum_i r_i^2(t)$, is a constant of the motion.[10] In a real plasma the radius could undergo small oscillations near the upper hybrid frequency, and we have averaged over these small fast oscillations here. In the simulations times are normalized to ω_z and distances to $(3e^2/M\omega_z^2)^{1/3}$, where ω_z is the frequency of axial oscillation of a single particle in the quadratic external trap potential. The magnetic field is chosen so that $\Omega=10\,\omega_z$. In a spherical cloud the plasma frequency is $\omega_p=\sqrt{3}\,\omega_z$.

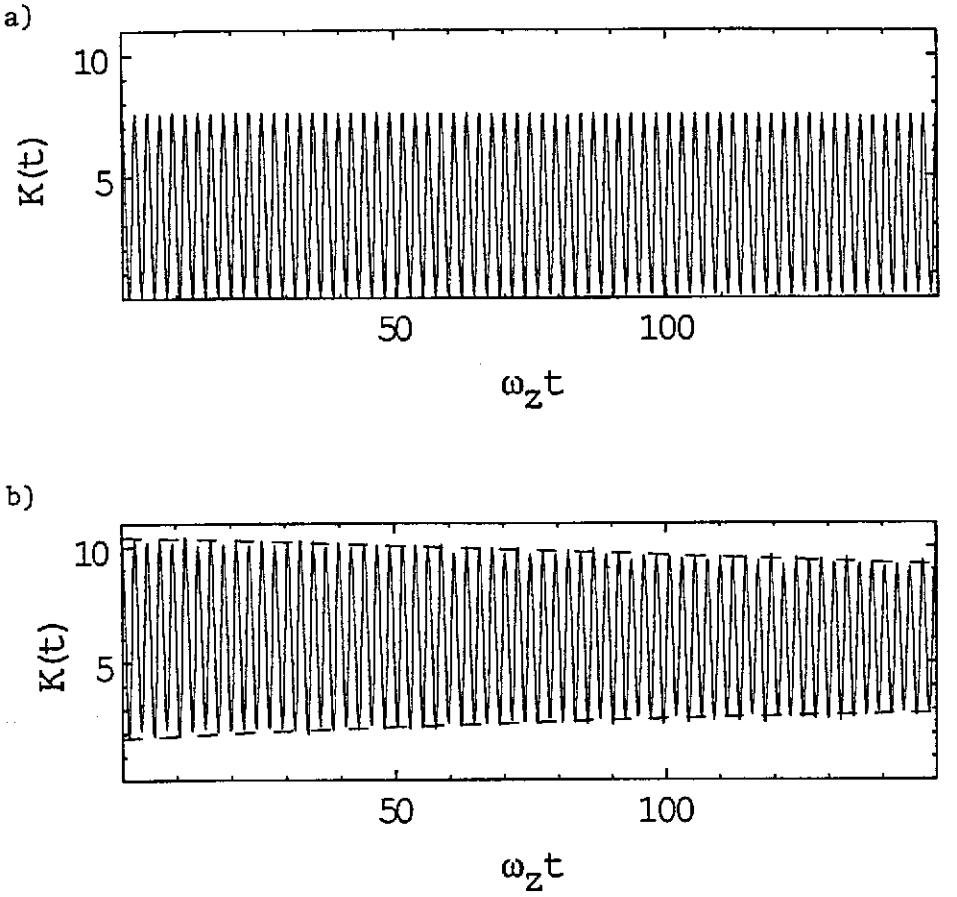

FIGURE 2

Molecular dynamics computer simulations of the (2,0) normal mode for an initially spherical cloud of 768 charges; $\Omega = 10\,\omega_z$. Kinetic energy $K(t)$ is plotted versus time. a) Initial $\Gamma = \infty$. Measured frequency over a period of $400\,\omega_z^{-1}$: $\omega_{20} = 1.3418\,\omega_z$. b) Initial $\Gamma = 90$. Measured frequency over a period of $400\,\omega_z^{-1}$: $\omega_{20} = 1.3423\,\omega_z$. The dashed line is the envelope obtained from the fit of Eq. (13), corresponding to $\gamma_1 = 0.001\,\omega_z$ and $\gamma_2 = 0.003\,\omega_z$.

In Fig. (2a) we plot the kinetic energy of the cloud, $K(t) \equiv \sum_i M v_{zi}^2(t)/2$, which varies at twice the mode frequency ω_{20} as the spheroid expands and contracts along the magnetic field. For this case the cloud of $N = 768$ charges was initially at zero temperature—i.e. in a crystallized state with $v_{zi}^{(0)} = 0$. The frequency of this oscillation in fluid theory is easily obtained from either Eq. (10) or Eq. (12) in the large Ω_c (guiding center) limit: $\omega_{20}^{th} = 3/\sqrt{5}\,\omega_z = 1.3416\,\omega_z$. This prediction matches the simulation to a part in 10^4, and there is little damping of the oscillation. This is because this fluid oscillation corresponds closely to one of the $3N$ normal modes of the crystal.

On the other hand, if we begin with a spherical plasma of $N = 768$ charges at $\Gamma \simeq 90$ the mode frequency remains within a part in 10^3 compared to the fluid theory, but there is measurable damping of the oscillation, and a concomitant increase in the thermal energy of the cloud (Fig. 2b). We fit $K(t)$ to the form

$$K(t) = A_1 e^{-2\gamma_1 t} \cos^2(\omega_{20} t) + A_2 (A_3 - e^{-2\gamma_2 t}) . \tag{13}$$

The term proportional to A_1 represents the kinetic energy in the mode damping at rate γ_1, while the term proportional to A_2 represents the thermal energy of the plasma. In Fig. 2a, $A_3 = 1$ and γ_1 and γ_2 are negligibly small, whereas in Fig. 2b a damping rate of $\gamma_1 = 0.001\,\omega_z$ and a heating rate of $\gamma_2 = 0.003\,\omega_z$ are observed.

It is interesting to note that this mode of oscillation is purely compressional in nature—there is no fluid shear induced by a (2,0) oscillation in the length of the spheroid, only a uniform compression. The observed damping is therefore a measure of the coefficient of bulk viscosity. The increase of viscous damping with decreasing

correlation is a common feature of viscoelastic systems, describable in simple models through introduction of a complex viscosity coefficient.[11] However, this phenomenon is unlike the behavior of weakly coupled plasmas where collisional viscosity decreases as temperature increases, and observation of this behavior may therefore be a useful experimental diagnostic of the strongly correlated state.

We are currently supplementing these preliminary results with more computer simulations in order to determine the scaling of the mode damping with plasma shape, particle number, magnetic field strength and Γ.

ACKNOWLEDGMENTS

This work was supported by the U.S. National Science Foundation under grant PHY 87-06358, the U.S. Office of Naval Research under grant N00014-89-J-1714, as well as a grant of supercomputer time from the San Diego Supercomputer Center. Portions of this work have been submitted to *Phys. Rev. A.*[12]

REFERENCES

1) Gilbert, S., J. Bollinger and D. Wineland, 1988, Phys. Rev. Lett. **60**, 2022.
2) Heinzen, D. *et al.*, 1991, Phys. Rev. Lett. **66**, 2080.
3) Malmberg, J.H. and T.M. O'Neil, 1977, Phys. Rev. Lett. **39**, 1071.
4) Driscoll, C.F., J.H. Malmberg and K.S. Fine, 1988, Phys. Rev. Lett. **60**, 1290.
5) Brewer, L.R. *et al.*, 1988, Phys. Rev. A **38**, 859.
6) Dubin, D.H.E., 1991, Phys. Rev. Lett. **66**, 2076.
7) Dubin, D.H.E., 1992, Phys. Fluids B (submitted).
8) Davidson, R.C. 1974, *Theory of Nonneutral Plasmas* (W.A. Benjamin: Reading, Mass.), p. 62.
9) This work is being performed in collaboration with J.P. Schiffer.
10) Dubin, D.H.E. and T.M. O'Neil, 1988, Phys. Rev. Lett. **60**, 1286.
11) Hansen, J.P. and I.R. McDonald, 1986, *Theory of Simple Liquids* (Academic Press: London), p. 293.
12) Bollinger, J.J., D.J. Heinzen, F.L. Moore, W.M. Itano, D.J. Wineland and D.H.E. Dubin, 1992, Phys. Rev. A. (submitted).